A Radar-Oriented Approach to the Normal Distributions Transform

Heller, Martijn ; Petrov, Nikita; Yarovoy, Alexander

DOI
10.23919/EuRAD50154.2022.9784492

Publication date
2022

Document Version
Final published version

Published in
Proceedings of the 18th European Radar Conference

A Radar-Oriented Approach to the Normal Distributions Transform

Martijn Heller, Nikita Petrov, Alexander Yarovoy

Microwave Sensing, Signals and Systems (MS3), Delft University of Technology, The Netherlands
martijn_heller@hotmail.com, {N.Petrov, A.Yarovoy}@tudelft.nl

***Abstract* — A modification of the scan-matching technique known as the Normal Distributions Transform to be applicable to radar data is presented. The proposed modification uses the measurements of received signal power to account for possible radar cross-section (RCS) fluctuation of the scene, which is prone to cause missed detections, undesirable in scan-matching techniques. It is demonstrated that RCS fluctuations according to a Swerling III model leads to an increase of the pose estimation errors, while the proposed approach reduces the errors to values equivalent to what can be achieved in the abscence of these fluctuations.**

***Keywords* — Scan-matching, Swerling, Normal Distributions Transform.**

I. Introduction

In the applications of highly and fully automated driving, high accuracy estimates of the vehicle's location are of utmost importance. The localization problem in unknown environment using range scanners is addressed in the framework of Simultaneous Localization and Mapping (SLAM). However, these techniques require data association and memorization of individual landmarks. Additionally, position estimates resulting from the SLAM approaches are known to drift over time due to increasing uncertainty.

An alternative approach is based on scan-matching techniques which use the point clouds that result from 2D or 3D range scans to estimate the relative pose. Range scans at two different time instances are considered, the so-called "reference scan" and the "current scan". The objective is to find the relative pose of the vehicle between these two scans that results in their maximum overlap. The scan-matching techniques can be divided into two main groups: the feature-based techniques and the distribution-based approaches.

Due to the popularity of both laser sensors and scan-matching techniques within the robotics community, the existing techniques are optimized for LiDAR measurements. Laser scanners, however, come at a higher cost [1] and perform poorly in bad weather conditions such as heavy rain or fog [2]. These shortcomings of laser sensors can be overcome with a complementary mm-wave radar available in the majority of cars with a high automation level. However, the existing scan-matching techniques, especially the feature-based approaches, perform poorly with radar data due to lower angular resolution of radar compared to LiDAR and frame-to-frame fluctuations of the radar response. The radar cross-section (RCS) of a target is highly dependent on the observation angle, especially in the case of a complex shape [3]. This in turn results in inconsistency in the reflected power of the same target after movement of the vehicle, which can result in missed detections in one of the scans used for scan-matching, causing the point clouds to suffer from "floating points" – the primitive detections which do not have a counterpart in the other scan. Because of this, the distribution-based approaches offer a more attractive solution.

Pioneering the distribution-based approaches is the Normal Distributions Transform (NDT) [4]. The NDT converts the 2D range scans from the native polar coordinate frame to Cartesian coordinates after which the reference scan is represented by a combination of bivariate Gaussian distributions related to the distribution of the points within the cells of a grid on the xy plane. In an effort to mitigate the influence of floating points in the NDT only grid cells that contain 3 or more points are used to construct the distribution. This, however, only partially addresses the target fluctuation issue.

In this paper we address the problem of RCS fluctuations in the application of the conventional NDT to radar data by incorporating knowledge about scene RCS into the localization problem. The structure of the paper is as follows: First, the principles of the NDT are explained in detail in Section II. Section III elaborates on the incorporation of knowledge about the RCS into the conventional NDT. Simulation results of this approach can be found in Section IV and verification using real data is presented in Section V. Finally, in Section VI conclusions are drawn.

II. The Normal Distributions Transform

The objective of scan-matching techniques is to find the relative pose $\mathbf{p}$ of the vehicle between the two sequential measurements of the environment, referred to as the "reference scan" and the "current scan". For plane geometry, the relative pose $\mathbf{p} = [t_x, t_y, \phi]^{\mathrm{T}}$ defines the translation of the vehicle between two scans along axes x and y (we consider that axis x aligns with the heading of the vehicle), together with the change of heading ϕ between the two scans.

The Normal Distributions Transform (NDT) is a scan-matching technique, which utilizes a combination of scaled Normal (Gaussian) distributions defined on a regular

subdivision of the plane to represent a scan. This piece-wise continuous and twice differentiable description of the map allows for formulation of the objective function over the relative pose $\mathbf{p}$ and minimizing it using Newton's method. The NDT algorithm is shortly described below; for more details the reader is referred to [4].

A. Scan Representation

The conventional implementation of NDT assumes that in each frame the sensor provides a point cloud in 2D Cartesian coordinates corresponding to the detector output. The sensors installed on a car – lidar, camera and radar – perceive the environment in polar coordinates; therefore polar to Cartesian coordinate transform is applied to the data first.

Then, the observed space around the vehicle is divided into equal cells on a regular grid in x and y coordinates. For each cell C_k in the grid containing a minimum of three points, the parameters of the bi-dimensional normal distribution – the mean vector $\mathbf{q}_k \in \mathbb{R}^{2\times 1}$ and the covariance matrix $\mathbf{\Sigma}_k \in \mathbb{R}^{2\times 2}$ – are calculated. The NDT representation of the reference scan therefore can be seen as a scaled PDF (or likelihood) of the Normal distribution in the grid cell k:

$$L(x,y) \propto \mathcal{N}\left([x,y]^T; \mathbf{q}_k, \mathbf{\Sigma}_k\right). \tag{1}$$

To minimize the effect of discretization, four overlapping grids are defined by shifting the original grid by half a cell in x coordinate, y coordinate and both respectively. The parameters $\mathbf{q}_k$ and $\mathbf{\Sigma}_k$ are estimated for each of them.

B. The Point Cloud Mapping Equations

The point cloud of the current scan can be mapped to the coordinates of the reference scan by applying a rotation and translation coordinate transform. The position of a point m after applying the pose change $\mathbf{p} = [t_x, t_y, \phi]^{\mathrm{T}}$ can be found through the mapping equations [4]:

$$\begin{aligned} x'_m &= x_m \cos(\phi) - y_m \sin(\phi) + t_x; \\ y'_m &= x_m \sin(\phi) + y_m \cos(\phi) + t_y, \end{aligned} \tag{2}$$

where $[x_m, y_m]$ are the coordinates of point m in the current scan, and $[x'_m, y'_m]$ are the coordinates of point m in the reference scan according to the pose change $\mathbf{p}$.

For each mapped point m the corresponding cell in the grid of the reference scan is found and a score is calculated as the value of the Normal probability density function at this point, the objective function of NDT optimization is then defined as a negative sum of the scores for each point in the current scan:

$$\min_{\mathbf{p}} \quad -\sum_{m=1}^{M} \exp\left[-\frac{(\mathbf{x}'_m - \mathbf{q}_k)^{\mathrm{T}} \mathbf{\Sigma}_k^{-1} (\mathbf{x}'_m - \mathbf{q}_k)}{2}\right], \tag{3}$$

for $\mathbf{x}'_m = [x'_m, y'_m]^{\mathrm{T}} \in C_k$. The negative sign is added to formulate a minimization problem to be solved for $\mathbf{p}$, which is involved in (3) through the coordinates mapping (2) of each point $\mathbf{x}'_m$.

C. The Optimization

The NDT optimization problem (3) is solved using the Newton's method. It requires the definition of the gradient and the Hessian of the objective function with respect to $\mathbf{p}$. Data representation via a combination of Normal distributions ensures that both gradient and Hessian of the objective function exist at any location within the scan. They are defined from the score per data point m as calculated through the expression inside the summation of (3) and can be found in [4]. The increment step is calculated by averaging gradient and Hessian matrices over the measured point cloud in the current scan and the four overlapping grids to obtain $\mathbf{g}$ and $\mathbf{H}$. At each iteration, the current scan point cloud is first transformed according to the mapping equations (2), then a single Newton step is taken to calculate the increment $\Delta\mathbf{p}$ by solving the following equation:

$$\mathbf{H}\Delta\mathbf{p} = -\mathbf{g} \tag{4}$$

$\Delta\mathbf{p}$ is added to the previous estimate of $\mathbf{p}$ to obtain a new pose estimate, to be used in the next iteration for mapping the point cloud. This process repeats until convergence.

III. Incorporation of knowledge about the RCS

The 3-point rule that is present in the calculation of the distribution guards the influence of floating points in LiDAR, however this is not sufficient for radar measurements. In radar measurements the received signal power is related to the radar cross section (RCS) of a target via the radar equation. Especially for complex targets, the RCS can fluctuate with a changing angle of incidence [3]. Because of the change of position of the radar scanner between the scans used for scan-matching, this RCS fluctuation can result in the reduction of the received power from an entire extended target below the detection threshold, causing a missed detection. This in turn causes floating points which are undesirable in scan-matching techniques. Such a problem is more prominent for targets whose received power is close to the detection threshold, i.e. weaker targets. By performing the scan-matching while putting more emphasis on stronger targets, this problem can be reduced.

Knowledge about the received power is available in radar scans through measurements of the Signal-to-Noise ratio (SNR). The incorporation of this knowledge can be implemented in two ways; by considering it in the calculation of the mean vectors and covariance matrices characterizing the piece-wise continuous distribution or by using it as a weighing factor for the score values of each point in calculation of the objective function (3).

A. Using SNR in the Calculation of the Distribution

In order to account for the SNR in the calculation of the distribution, the weighted mean and covariance are calculated. This results in the following relations:

$$\mathbf{q}_k^i = \frac{1}{W_k} \sum_{m=1}^{M_k} w_m \mathbf{x}_m^i, \tag{5}$$

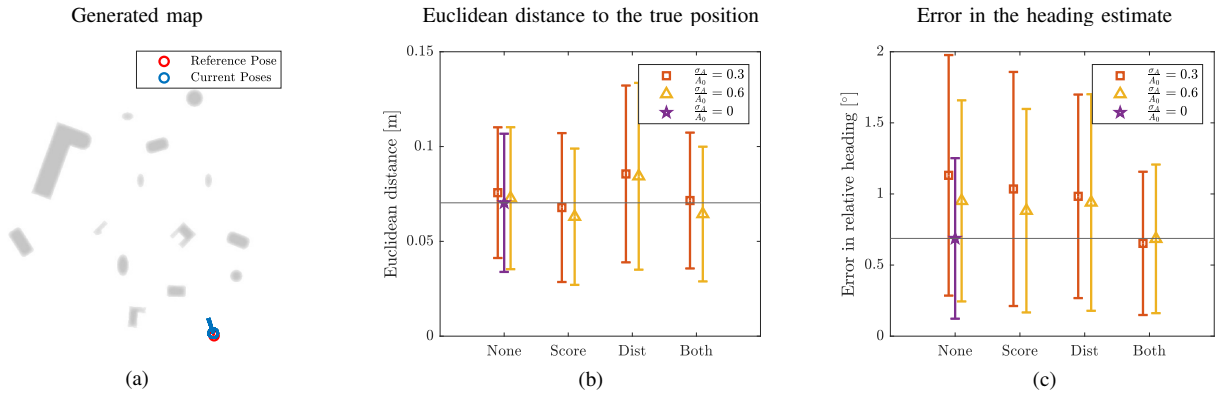

(a) (b) (c)

Fig. 1. Simulation results, (a) Set-up of the simulation, (b) Euclidean distance to the correct position, (c) error in the relative heading

$$\mathbf{\Sigma}_k^{i,j} = \frac{1}{W_k} \sum_{m=1}^{M_k} w_m (\mathbf{x}_m^i - \mathbf{q}_k^i)(\mathbf{x}_m^j - \mathbf{q}_k^j). \tag{6}$$

In these definitions, i and j denote the entries of the vector and matrix, m denotes the measured target whose associated weight w_m is defined as the received power, M_k is the total number of points inside C_k and $W_k = \sum_{m=1}^{M_k} w_m$.

B. Using SNR in Calculation of the Score

The same weight can be used in the calculation of the score, which results in the following minimization problem:

$$\min_{\mathbf{p}} \quad -\sum_{m=1}^{M} w_m \exp\left[-\frac{(\mathbf{x}'_m - \mathbf{q}_k)^{\mathrm{T}} \mathbf{\Sigma}_k^{-1} (\mathbf{x}'_m - \mathbf{q}_k)}{2}\right], \tag{7}$$

with the weight factors w_m defined in the same way as in (5), (6). This scaling with w_m is a linear operation, it is thus trivial to include it in the Hessian and gradient for the optimization.

IV. Simulations

In order to show the influence of the incorporation of knowledge about the RCS a simulation was set up to generate measurements of objects in front of an automotive radar.

A. Set-up of the Simulations

The measurements are simulated as if they were received by a 3 Tx $\times$ 4 Rx automotive radar, capable of measuring at a range resolution of $\Delta R \approx 17$ cm and a Doppler resolution $\Delta v \approx 0.08$ m/s. A comparison is made for different levels of RCS fluctuation corresponding to a Swerling III target model, simulated by modeling the received signal magnitude as a $Rice(A_0, \sigma_A)$ distributed variable [5]. The comparison is made for values $\frac{\sigma_A}{A_0} = 0.3$ and $\frac{\sigma_A}{A_0} = 0.6$, which puts the KLD of Swerling III versus Rician below 0.05. As a reference the results of measurements without RCS fluctuation ($\frac{\sigma_A}{A_0} = 0$) where the incorporation of knowledge about the RCS is not included in the algorithm is presented.

Within the map of Figure 1a a starting pose is chosen, whose scan will be used as the reference scan, and 50 relative poses are generated that are consistent with linear vehicle motion with nearly constant velocity at approximately 15 km/h with random fluctuation in the steering. Both the velocity and the steering fluctuations are simulated as Gaussian noise, characterized by a standard deviation $\sigma_v = 0.1$ km/h and $\sigma_\phi = 1°$, respectively. From each of the resulting positions radar scans are generated and used as the current scans in the scan-matching approach.

B. Results of the Simulations

The root mean square value of the Euclidean distance between the estimated positions and the actual positions and the root mean square error (RMSE) of the headings along with the standard deviation of these errors for each of the RCS incorporation methods for both of the investigated levels of RCS fluctuation are shown in Figure 1.The figure additionally shows the performance of the conventional NDT in abscence of RCS fluctuation and without incorporation of the RCS knowledge in the algorithm.

The results show that the position estimate does not suffer much from the increased level of RCS fluctuation, whereas the estimate of the relative heading does. Moreover, the incorporation of knowledge about the RCS reduces the increased error in the heading estimate to the same level as it would be without RCS fluctuation.

V. Experiment

For experimental verification measurements were made using a commercially available automotive radar attached to the front of a car. During the experiment, raw radar data with synchronized GPS locations were recorded, all processing was performed offline. This section describes the experiment set-up along with the results.

A. Set-up of the Experiment

For collection of the data the automotive radar operated at a center frequency of 77 GHz. The radar system contains a 3 Tx $\times$ 4 Rx MIMO array operating at a bandwidth of 860 MHz. The angular resolution is approximately $\Delta\theta = 8°$, the range resolution is $\Delta R = 0.1738$ m and the Doppler resolution is $\Delta v \approx 0.04$ m/s. The maximum measurable range is $R_{max} = 94$ m and the field of view of the radar is $\pm 60°$. During the experiment, the car was driving at approximately $v_{car} = 15$ km/h on a quiet piece of road on the TU Delft campus. The

collected data was pre-processed into a range-angle-Doppler data cube after which median detection was performed. In order to filter out any non-stationary targets, the vehicle velocity was estimated for each detected target m within a scan by rewriting the relation between a stationary target's measured relative Doppler velocity and its angle: $\hat{v}_{car,m} = v_m/\cos(\theta_m)$, after which the median value was taken over these calculated values. Using this estimate of the velocity, non-stationary targets were filtered out by discarding any target m that did not meet the criterion $|v_m - \hat{v}_{car}\cos(\theta_m)| < 0.5$ m/s.

B. Results of the Experiment

Since GPS data does not provide an accurate ground-truth of the local poses, the estimated poses are used to construct a global trajectory, which in turn is compared visually to the trajectory of the GPS. The construction of the trajectories is performed after crude filtering of outliers, by enforcing a bound on each of the estimation parameters. In case one of the parameters of the estimated pose is outside of this bound[1], the estimated pose is replaced with the position estimate of the previous timeframe along with a change in heading of $\phi = 0$. The resulting trajectories for 150 consecutive matched scans can be found in Figure 2. The black lines denote the estimated trajectories for each time frame, the shapes and bars denote the global pose at intervals of 10 timeframes.

From this figure it is clear that by not taking into account knowledge of the RCS the trajectory diverges considerably, whereas this problem is minimized for the other approaches. Each of the techniques underestimate the traveled distance compared to the GPS data. This is due to a problem in the synchronization between radar and GPS during the collection of the data. When looking at the average velocity needed to traverse the distance measured by the GPS within any timeframe it is seen that this value is approximately $0.5-1$ m/s higher than the instructed speed that was driven at during the experiment. This is further corroborated by the vehicle velocity estimates via the Doppler measurements. The difference in traversed distance between the trajectory according to the GPS and the estimated trajectories is approximately 13 meters. This is in line with the higher velocity of the GPS data over the 150 frames (15 seconds).

VI. Conclusion

A way to incorporate knowledge about the Radar cross-section (RCS) of a target in the existing scan-matching approach known as the Normal Distributions Transform (NDT) is proposed. It is shown that without incorporation of this knowledge, frame-to-frame RCS fluctuation according to a Swerling III model causes a considerable reduction in performance of the NDT as applied to radar measurements, especially with regards to the estimation of the relative heading. The RCS fluctuations cause missed detections, which in turn lead to the introduction of so-called floating points, i.e. detections in one scan that are not present in the other. With the availability of SNR measurements in radar scans, a reference to a target's RCS is obtained. This reference can be used to structure the solution of the NDT in such a manner that more emphasis is put on stronger targets, whose RCS fluctuations are less prone to cause floating points. It is shown using simulation data that by taking into account this knowledge of the RCS the estimation error resulting from the application of the NDT to radar scans subject to Swerling III fluctuations is brought back to a value identical to what can be achieved in the abscence of RCS fluctuation. Further it is shown through experimental data that not taking into consideration this knowledge results in divergence of the trajectory as reconstructed using the individual pose estimates. This problem is minimized when taking into account the RCS knowledge.

[1] chosen to be $t_{x,max} = 75$ cm, $t_{y,max} = 20$ cm and $\phi_{max} = 10°$

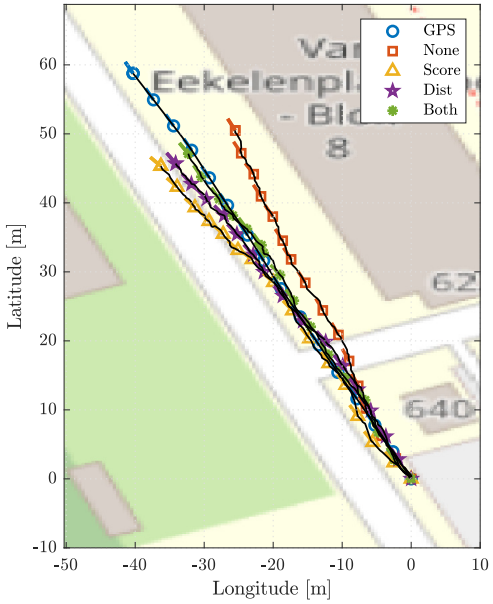

Fig. 2. The reconstructed trajectories using the individual pose estimates with as a reference the trajectory according to GPS

References

[1] S. Campbell, N. O'Mahony, L. Krpalcova, D. Riordan, J. Walsh, A. Murphy, and C. Ryan, "Sensor Technology in Autonomous Vehicles: A review," in *2018 29th Irish Signals and Systems Conference (ISSC)*, 2018, pp. 1–4.

[2] M. Kutila, P. Pyykönen, H. Holzhüter, M. Colomb, and P. Duthon, "Automotive LiDAR Performance Verification in Fog and Rain," in *2018 21st International Conference on Intelligent Transportation Systems (ITSC)*, 2018, pp. 1695–1701.

[3] M. A. Richards, J. A. Scheer, and W. A. Holm, *Principles of Modern Radar, Volume I - Basic Principles*. SciTech Publishing, 2010.

[4] P. Biber and W. Strasser, "The Normal Distributions Transform: a New Approach to Laser Scan Matching," in *Proceedings 2003 IEEE/RSJ International Conference on Intelligent Robots and Systems (IROS 2003) (Cat. No.03CH37453)*, vol. 3, 2003, pp. 2743–2748 vol.3.

[5] X. Song, W. D. Blair, P. Willett, and S. Zhou, "Dominant-plus-Rayleigh Models for RCS: Swerling III/IV versus Rician," *IEEE Transactions on Aerospace and Electronic Systems*, vol. 49, no. 3, pp. 2058–2064, 2013.